Osteoclasts promote the formation of hematopoietic stem cell niches in the bone marrow

Anna Mansour,[1,2] Grazia Abou-Ezzi,[1,3] Ewa Sitnicka,[4] Sten Eirik W. Jacobsen,[4,5] Abdelilah Wakkach,[1,3] Claudine Blin-Wakkach[1,3]

[1]Université de Nice Sophia Antipolis, 06000 Nice, France
[2]Centre National de la Recherche Scientifique, UMR 6235, Faculté de Médecine, 06100 Nice, France
[3]Institut National de la Santé et de la Recherche Médicale, UMR 576, Hôpital de l'Archet, 06202 Nice, France
[4]Hematopoietic Stem Cell Laboratory, Lund Research Center for Stem Cell Biology and Cell Therapy, Lund University, 22184 Lund, Sweden
[5]Haematopoietic Stem Cell Laboratory, Weatherall Institute of Molecular Medicine, John Radcliffe Hospital, University of Oxford, Oxford OX3 9DS, England, UK

Formation of the hematopoietic stem cell (HSC) niche in bone marrow (BM) is tightly associated with endochondral ossification, but little is known about the mechanisms involved. We used the *oc/oc* mouse, a mouse model with impaired endochondral ossification caused by a loss of osteoclast (OCL) activity, to investigate the role of osteoblasts (OBLs) and OCLs in the HSC niche formation. The absence of OCL activity resulted in a defective HSC niche associated with an increased proportion of mesenchymal progenitors but reduced osteoblastic differentiation, leading to impaired HSC homing to the BM. Restoration of OCL activity reversed the defect in HSC niche formation. Our data demonstrate that OBLs are required for establishing HSC niches and that osteoblastic development is induced by OCLs. These findings broaden our knowledge of the HSC niche formation, which is critical for understanding normal and pathological hematopoiesis.

CORRESPONDENCE
Claudine Blin-Wakkach:
blin@unice.fr

Abbreviations used: Ang-1, angiopoietin 1; HSC, hematopoietic stem cell; Jag-1, Jagged 1; Kit-L, Kit ligand; LSK, $Lin^{neg}Sca1^{+}cKit^{+}$; OBL osteoblast; OCL, osteoclast; OPN, osteopontin; SDF1, tromal-derived factor-1; ZA, zoledronic acid.

In adults, hematopoietic stem cells (HSCs) reside in specialized niches located in the BM. Cellular components and mechanisms involved in these niches are under extensive investigations, but most of them are performed in the context of HSC mobilization in adults, and little is known about the initial formation of the HSC niche.

During vertebrate ontogeny, hematopoiesis progresses in different anatomical sites to become predominant in the BM in adults (Aguila and Rowe, 2005). Endochondral ossification precedes the appearance of HSCs in the BM and is required for the formation of their niche (Chan et al., 2009), but the precise mechanisms remain to be determined. HSCs reside in the endosteal region, at the interface between the bone and BM, in a region of active bone remodeling (Kollet et al., 2007). HSCs are known to express calcium-sensing receptors involved in retaining them close to endosteal surfaces where calcium concentration is very high because of the activity of osteoclasts (OCLs) and osteoblasts (OBLs; Adams et al., 2006). Thus, bone modeling and remodeling are likely to be involved in the modulation or the formation of the endosteal HSC niche.

Bone modeling and remodeling are highly regulated processes involving complex interactions between the bone-forming OBLs and the bone resorbing OCLs. These interactions involve cellular contacts, the production of cytokines, and the generation of coupling factors during bone resorption (Martin and Sims, 2005). OBLs and other mesenchymal cells, such as perivascular primitive mesenchymal cells (Nilsson et al., 2001; Calvi et al., 2003; Zhang et al., 2003; Visnjic et al., 2004; Morikawa et al., 2009; Méndez-Ferrer et al., 2010; Raaijmakers et al., 2010), provide niches where HSCs are exposed to molecular

G. Abou-Ezzi, A. Wakkach, and C. Blin-Wakkach's present address is Centre National de la Recherche Scientifique, LP2M, FRE 3472, Parc Valrose, 06100 Nice, France.

The Rockefeller University Press $30.00
J. Exp. Med. Vol. 209 No. 3 537-549
www.jem.org/cgi/doi/10.1084/jem.20110994

The Journal of Experimental Medicine

signals, such as cytokines, chemokines, and growth factors, that control their fate in terms of self-renewal, proliferation, apoptosis, differentiation, homing, quiescence, etc. (Adams and Scadden, 2006). In adults, selective depletion of OBLs leads to a reduction in HSC number (Visnjic et al., 2004), whereas an increase in OBL number is associated with an augmentation of the HSC pool size in the BM (Calvi et al., 2003). This effect of OBLs is caused in part by direct cell interactions with HSCs. Signaling through Jagged 1 (Jag-1) on OBLs and its receptor Notch on HSCs is involved in the expansion of the HSC pool (Calvi et al., 2003), and signaling through stromal Angiopoietin 1 (Ang-1) and its receptor Tie-2 on HSCs is involved in maintaining HSC quiescence in the niche (Arai et al., 2004). OBLs and mesenchymal cells also express osteopontin (OPN), which is a negative regulator of HSC pool size that inhibits HSC proliferation, promotes HSC apoptosis, and affects the expression of Jag-1 and Ang-1 by stromal cells (Nilsson et al., 2005; Stier et al., 2005). Stromal-derived factor-1 (SDF-1), which is produced by mesenchymal cells and OBLs, is the major chemoattractant for many hematopoietic progenitors, including HSCs (Dar et al., 2006). Mice deficient in SDF-1 or its receptor CXCR4 display normal fetal hematopoiesis in the liver, but lack BM engraftment by hematopoietic cells (Nagasawa et al., 1996; Peled et al., 1999). All these data underline the essential role of mesenchymal cells and OBLs in the BM HSC niche.

OCLs have been implicated in HSC mobilization in response to stress or pharmacological treatments such as G-CSF (Lévesque et al., 2010), but the mechanisms involved are less characterized. OCL activation increases the stress-induced mobilization of HSCs by producing proteolytic enzymes that cleave factors involved in the HSC niche (Kollet et al., 2006; Cho et al., 2010). OCL inhibition also increases HSC mobilization in response to G-CSF (Takamatsu et al., 1998; Winkler et al., 2010; Miyamoto et al., 2011) and reduces the number of primitive HSCs in the BM (Lymperi et al., 2011). Therefore, modulation of OCL activity appears to alter the response of the HSC niche to mobilizating agents once this niche is established. Interestingly, mice lacking OCL activity develop severe osteopetrosis, whch is associated with extramedullary hematopoiesis, suggesting that OCLs may participate not only in the regulation or maintenance but also in the initial formation of the HSC niche (Dougall et al., 1999; Kong et al., 1999; Tagaya et al., 2000; Blin-Wakkach et al., 2004b). However, to our knowledge, characterization of the HSC compartment and HSC niches in the BM of osteopetrotic mice has never been reported.

To better understand how bone resorption can affect the formation of the HSC niche, we used the *oc/oc* mouse model, which develops a very severe form of osteopetrosis and displays severe alterations in hematopoiesis (Blin-Wakkach et al., 2004b). In these mice, OCLs are inactive because of a mutation in the *Tcirg1* gene (Scimeca et al., 2000). This gene encodes the a3 subunit of the vacuolar-ATPase, which is necessary for proton production by OCLs and is not expressed by OBLs (Schinke et al., 2009). In addition to a severe alteration in endochondral ossification, we herein show that the absence of OCL activity results in a defective formation of the HSC niche in the BM, leading to retention of HSCs in the spleen. This defect includes a modification of the phenotype of mesenchymal cells involved in the HSC niche, in particular a reduced OBL differentiation, as well as a dramatic decrease in the expression of the main regulators of the HSC niche. Furthermore, we demonstrate that the specific restoration of OCL function in *oc/oc* mice leads to the recovery of the mesenchymal cell phenotype and function, and the restoration of the HSC niche leading to normal HSC homing in the BM. Our data demonstrate for the first time that OCLs promote the formation of the HSC niche by controlling the maturation of OBLs that participate in this niche.

RESULTS

Dramatic reduction of the HSC pool in the BM of *oc/oc* mice

In *oc/oc* mice, the bone phenotype is dramatically altered by the absence of OCL activity, and BM cellularity is dramatically reduced (Seifert and Marks, 1985; Blin-Wakkach et al., 2006b; Wakkach et al., 2008). Despite the profound alterations in hematopoiesis described in these mice (Blin-Wakkach et al., 2004a,b), their HSC

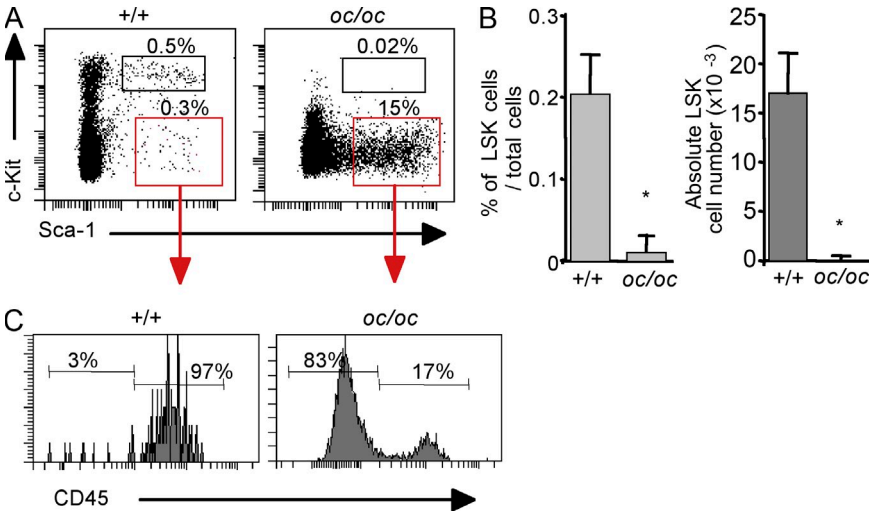

Figure 1. The HSC pool is dramatically reduced in the *oc/oc* BM. (A) Flow cytometry analysis of LSK cells in BM of 17-d-old *oc/oc* and control littermates gated on Lin^{neg} cells. Gating and percentage of the LSK cells are indicated. (B) The percentage and the absolute number of BM LSK cells from the hind legs was determined and presented as the mean ± SD from six mice per group. *, $P < 0.01$. (C) Analysis of CD45 expression within the $Lin^{neg}Sca1^{+}c\text{-}kit^{neg}$ BM population. Data are representative of those obtained for six mice in each group and three independent experiments.

compartment has never been analyzed in the BM. Therefore, we analyzed the Lin^{neg}Sca1^{+}cKit^{+} (LSK) hematopoietic stem/progenitor cell compartment by flow cytometry. The frequency and absolute number of LSK cells was decreased by 90 and 99.8%, respectively, in the BM of *oc/oc* mice compared with controls (Fig. 1, A and B). Interestingly, this near absence of LSK cells was accompanied by the accumulation of a Lin^{neg}Sca1^{+}cKit^{neg} population in the BM of *oc/oc* mice (Fig. 1 A). Analysis of this population revealed that ~80% of these cells did not express the panhematopoietic marker CD45, suggesting that they represent mesenchymal cells (Fig. 1 C). On the contrary, in the wild-type control mice, the Lin^{neg}Sca1^{+}cKit^{neg} cells present in the BM belonged to the CD45^{+} hematopoietic cell population (Fig. 1 C).

Altered mesenchymal cell phenotype and defective HSC niche in the BM of *oc/oc* mice

Mesenchymal cells are key components of the HSC niche. Therefore, the dramatic decrease in the HSC pool size in the *oc/oc* BM could be related to modifications in mesenchymal cell populations, as suggested by the accumulation of the CD 45^{neg}Lin^{neg}Sca1^{+}cKit^{neg} population. To address this question, we further analyzed the phenotype of TER119^{neg}CD45^{neg} mesenchymal cells present in the BM of *oc/oc* mice. Mesenchymal cells represented ~20% of total BM cells in normal mice (Fig. 2 A). In *oc/oc* mice, TER119^{neg}CD45^{neg} mesenchymal cells represent 80% of total BM cells, the majority of them coexpressing the progenitor cell marker Sca1 (Fig. 2, A and B). Indeed, flow cytometric analysis revealed a 10-fold increase in the proportion of TER119^{neg}CD45^{neg}Sca1^{+} mesenchymal cells in the BM of *oc/oc* mice compared with the controls, whereas the percentage of TER119^{neg} CD45^{neg} Sca1^{neg} cells was equal in both mouse genotypes (Fig. 2 B). These data suggest that the mesenchymal cells present in *oc/oc* mice are mainly progenitor cells. The link between the decreased OCL activity and the alteration of the LSK and mesenchymal cell compartments was confirmed in newborn +/+ mice treated with zoledronic acid (ZA), a bisphosphonate that inhibits OCL activity (Russell et al., 2008). In ZA-treated mice, the LSK cell pool was decreased in association with an increased proportion of Lin^{neg}Sca1^{+}cKit^{neg} CD45^{neg} mesenchymal progenitors (Fig. 2 C), as observed in the *oc/oc* BM (Fig. 1 C). Similar results were also observed in newborn +/+ mice treated with calcitonin, another OCL inhibitor (unpublished data). Altogether, these data strongly suggest that reduced OCL function affects the BM HSC niche.

To gain more insight into the phenotype of the *oc/oc* CD45^{neg} mesenchymal cells, we analyzed the expression of genes involved in regulation of HSC maintenance and homing in the BM. The expression of *Ang-1*, *Jag-1*, *Sdf1*, and *Kit ligand (Kit-L)* was dramatically decreased in CD45^{neg} cells from the *oc/oc* BM compared with the controls, whereas no significant difference was observed in *N-Cad* expression (Fig. 3 A). Interestingly, expression of *Opn*, a negative regulator of the HSC pool, was significantly higher in *oc/oc* mesenchymal cells compared with the control cells (Fig. 3 A). Altogether, these results demonstrate that the BM mesenchymal compartment was highly altered in *oc/oc* mice, and suggest its impairment in supporting hematopoietic stem/progenitor cell homing and retention.

To address this hypothesis, we performed an in vitro migration assay. Using transwell chambers, we showed that

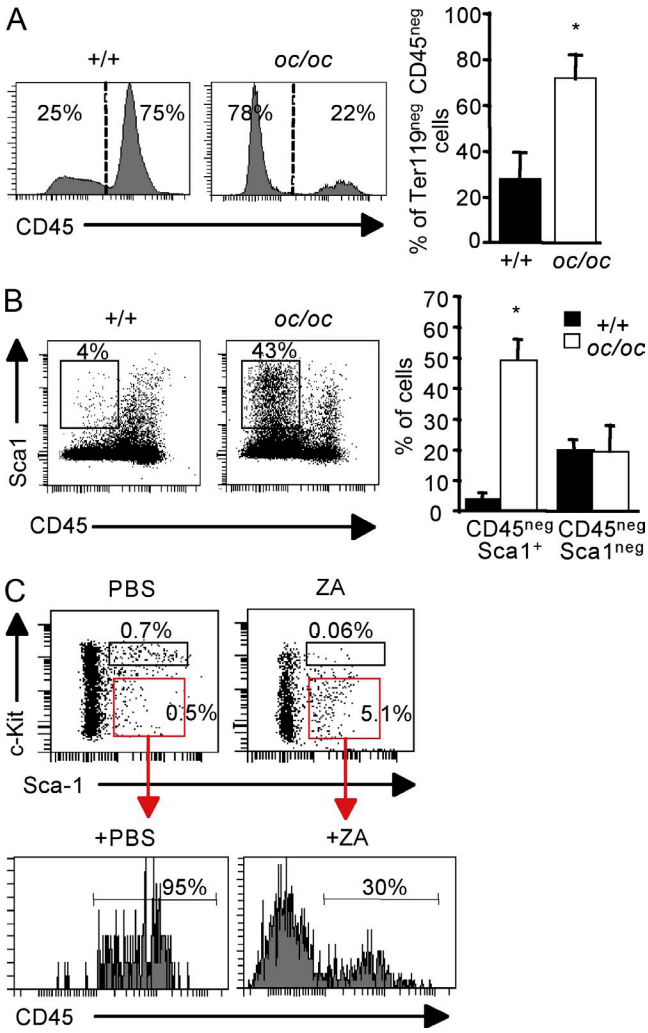

Figure 2. Phenotype of the mesenchymal cells from the BM of *oc/oc* mice. (A) Flow cytometry analysis of BM Ter119^{neg}CD45^{neg} mesenchymal cells. Bar graph shows the mean ± SD of the percentage of mesenchymal Ter119^{neg}CD45^{neg} cells obtained from 6 17-d-old *oc/oc* and control littermates per group and is representative of 2 independent experiments. *, $P < 0.01$. (B) Flow cytometry analysis of CD45 and Sca1 expression in Ter119^{neg} BM cells from +/+ and *oc/oc* mice. Bar graph shows represents the mean ± SD of the percentage of cell populations obtained for 6 mice per group and are representative of 2 independent experiments. *, $P < 0.01$. (C) Flow cytometry analysis of LSK (top) and Lin^{neg}Sca1^{+}c-kit^{neg} (bottom) cells in the BM of 15-d-old +/+ mice treated with PBS or ZA. Data are representative of those obtained for three mice in each group in two independent experiments.

the CD45^{neg} cells from *oc/oc* mice displayed a fourfold-reduced ability to attract LSK cells compared with those from the wild-type mice (Fig. 3 B). This result was further confirmed by in vivo assay where LSK cells from actin-GFP mice were injected into 2-d-old irradiated *oc/oc* and wild-type mice. 18 h after this transfer, the localization of GFP$^+$ progenitors was investigated by flow cytometry, in the BM, spleen, and blood. As expected, in +/+ mice, the transferred GFP$^+$ cells localized mainly in the BM compared with the spleen (Fig. 3 C). In contrast, homing of transferred GFP$^+$ LSK cells into the *oc/oc* BM was >10-fold reduced compared with the control mice and the majority of injected GFP$^+$ cells were located in the spleen or in the blood (Fig. 3 C). Moreover, analysis of endogenous LSK cells revealed that their proportion was increased in the spleen (Fig. 3 D) and liver (not depicted) of *oc/oc* mice compared with the controls. Collectively, these data confirmed that the *oc/oc* BM environment does not support LSK cell homing and that other perinatal hematopoietic organs such as the spleen and liver can represent alternative sites for hematopoiesis in *oc/oc* mice, as previously suggested (Blin-Wakkach et al., 2004b).

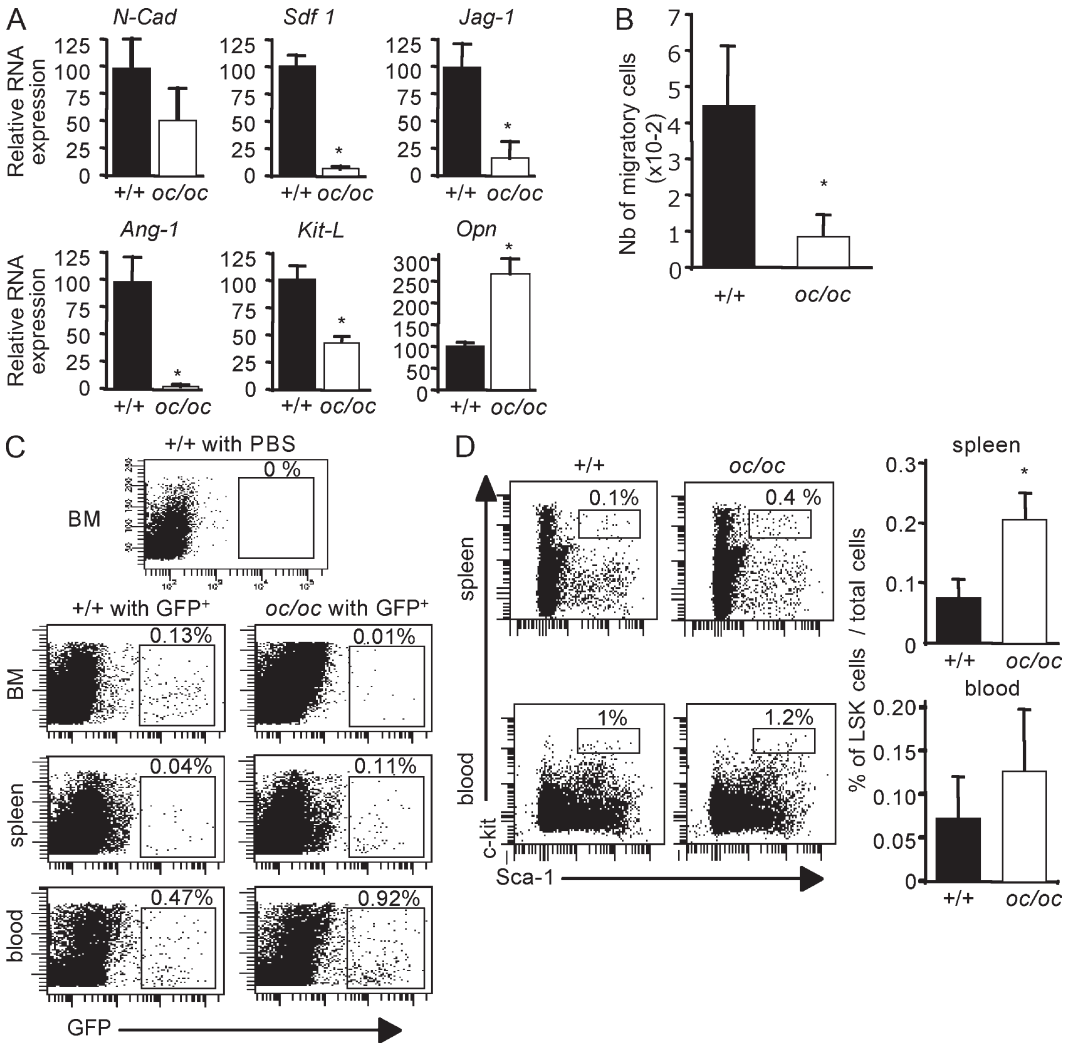

Figure 3. Impaired homing of hematopoietic progenitors in *oc/oc* mice. (A) Real-time RT-PCR analysis on CD45^{neg} cells sorted from the BM of *oc/oc* and wild-type mice. Ct values were normalized to the 36B4 RNA. Differences were calculated with the $2^{-\Delta Ct}$ method and expressed as the percentage relative to the values obtained for the +/+ cells. Results are presented as the mean ± SD of triplicates from 10 *oc/oc* and 5 +/+ mice. *, $P < 0.01$. (B) In vitro migration assay of LSK cells sorted from the BM of actin-GFP (3–4-wk-old) mice in response to CD45^{neg} mesenchymal cells sorted from the BM of *oc/oc* and +/+ littermate (17-d-old) mice. Results are presented as the mean ± SD of triplicates of cells pooled from three *oc/oc* and three wild-type mice and are representative of two independent experiments. *, $P < 0.05$. (C) In vivo homing analysis of LSK sorted from the BM of actin-GFP mice and injected (2.5×10^5 cells) into newborn *oc/oc* and control mice. Analysis of GFP$^+$ cells was performed 18 h after cell transfer. Percentages of GFP$^+$ cells are indicated. The data are representative of three *oc/oc* and control mice and two independent experiments. (D) Flow cytometry analysis of LSK cells in the spleen and the blood of 17-d-old +/+ and *oc/oc* mice. Cells were gated on Lin^{neg} cells. Percentage of LSK cells is indicated. Bar graphs show the mean ± SD of LSK cell percentage obtained for six mice per group and are representative of two independent experiments. *, $P < 0.01$.

The defect in the oc/oc HSC niche is associated with a reduced osteoblastic commitment

In the BM, HSCs reside in endosteal niches, in close association with OBLs, and also in perivascular niches, in proximity to BM sinusoidal vessels (Nilsson et al., 2001; Calvi et al., 2003; Zhang et al., 2003; Visnjic et al., 2004; Morikawa et al., 2009; Méndez-Ferrer et al., 2010). Therefore, we examined both components of the niche in the *oc/oc* BM. Flow cytometric analysis demonstrated that the TER119^{neg}CD45^{neg}Sca1^{+} population from the *oc/oc* BM contained the same proportion of CD44^{+} cells, whereas the proportion of cells expressing integrin α5 (CD49e) was reduced (Fig. 4 A). Interestingly, the percentage of TER119^{neg} CD45^{neg} mesenchymal cells expressing CD51 was also reduced (Fig. 4 A). Because CD49e expression has been associated with OBL lineage commitment (Hamidouche et al., 2009) and CD51 is a marker for OBLs (Lundberg et al., 2007), these results indicate that the OBL differentiation is impaired in *oc/oc* mice. This was confirmed by real time RT-PCR analysis of the expression of the main OBL markers in the CD45^{neg} cells purified from the BM of *oc/oc* and control mice. Expression of *Runx2*, a master gene of OBL differentiation, as well as *alkaline phosphatase* (*Alp*), *osteocalcin*, and *Bone sialoprotein* (*Bsp*) was significantly reduced in the CD45^{neg} mesenchymal cells from *oc/oc* mice, compared with the controls (Fig. 4 B). These results confirmed recently published data showing an increased number of colony forming unit–fibroblast (CFU-F)–representing mesenchymal cells, but a decreased CFU-ALP–representing OBLs, in the BM of *oc/oc* mice (Mansour et al., 2011). Altogether, these findings confirmed a reduced OBL commitment and differentiation in *oc/oc* mice.

We also analyzed the perivascular primitive mesenchymal cells present in *oc/oc* BM marrow using the recently described marker platelet-derived growth factor receptor α (PDGFRα; Morikawa et al., 2009). The frequency of PDGFRα^{+} cells was significantly higher in mesenchymal progenitors from *oc/oc* mice compared with the controls (Fig. 4 A). The function of perivascular mesenchymal cells and OBLs in maintaining the HSC niche is regulated by macrophages (Winkler et al., 2010; Chow et al., 2011; Christopher et al., 2011). As macrophages arise from the same progenitor as OCLs, we wondered if the increase in OCL numbers observed in *oc/oc* mice was detrimental to the differentiation of macrophages, resulting in a reduced retention of HSCs in the BM. The percentage of CD11b^{+}F4/80^{+}Ly6G^{+} and F4/80^{+}CD115^{+}Gr1^{neg}CD169^{+}

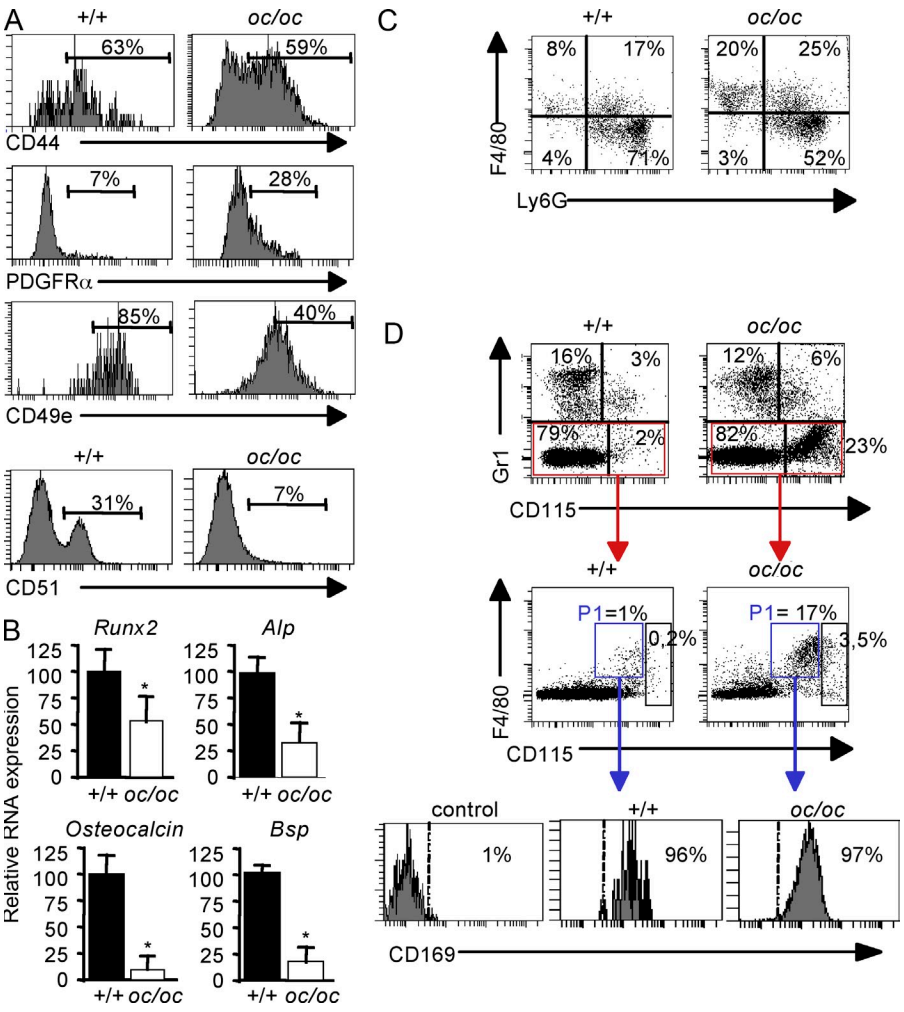

Figure 4. Reduced osteoblastic commitment in the BM of *oc/oc* mice. (A) Flow cytometry analysis showing CD44, PDGFRα, CD49e expression on Ter119^{neg}CD45^{neg}Sca1^{+} cells and CD51 expression on Ter119^{neg}CD45^{neg} cells from the BM of *oc/oc* and wild-type mice. Percentages of the populations are indicated, and the data are representative of three mice per group and two independent experiments. (B) Real-time RT-PCR analysis of *Runx2*, *Alp*, *Osteocalcin*, and *Bsp* expression in CD45^{neg} cells sorted from the BM of *oc/oc* and wild-type mice. Ct values were normalized to the 36B4 RNA. Differences were calculated with the $2^{-\Delta Ct}$ method and expressed as the percentage relative to the values obtained for the wild-type cells. Results are presented as the mean ± SD of triplicates from 10 *oc/oc* and 5 wild-type mice. *, $P < 0.01$. (C) Flow cytometry analysis of F4/80^{+} and Ly6G^{+} macrophages populations in the BM of *oc/oc* and +/+ mice. Cells were gated on CD11b^{+} cells. Percentages of the populations are indicated and are representative of those obtained from three mice per group and two independent experiments. (D) Flow cytometry analysis of F4/80^{+}CD115^{+}Gr1^{neg}CD169^{+} macrophages in the BM of *oc/oc* and +/+ mice. Cells were gated on total BM cells (top), on Gr1^{neg} cells (middle) and on Gr1^{neg} F4/80^{+}CD115^{+}SSC$^{int/low}$ cells. Percentages of the populations are indicated and are representative of those obtained from three mice per group and two independent experiments.

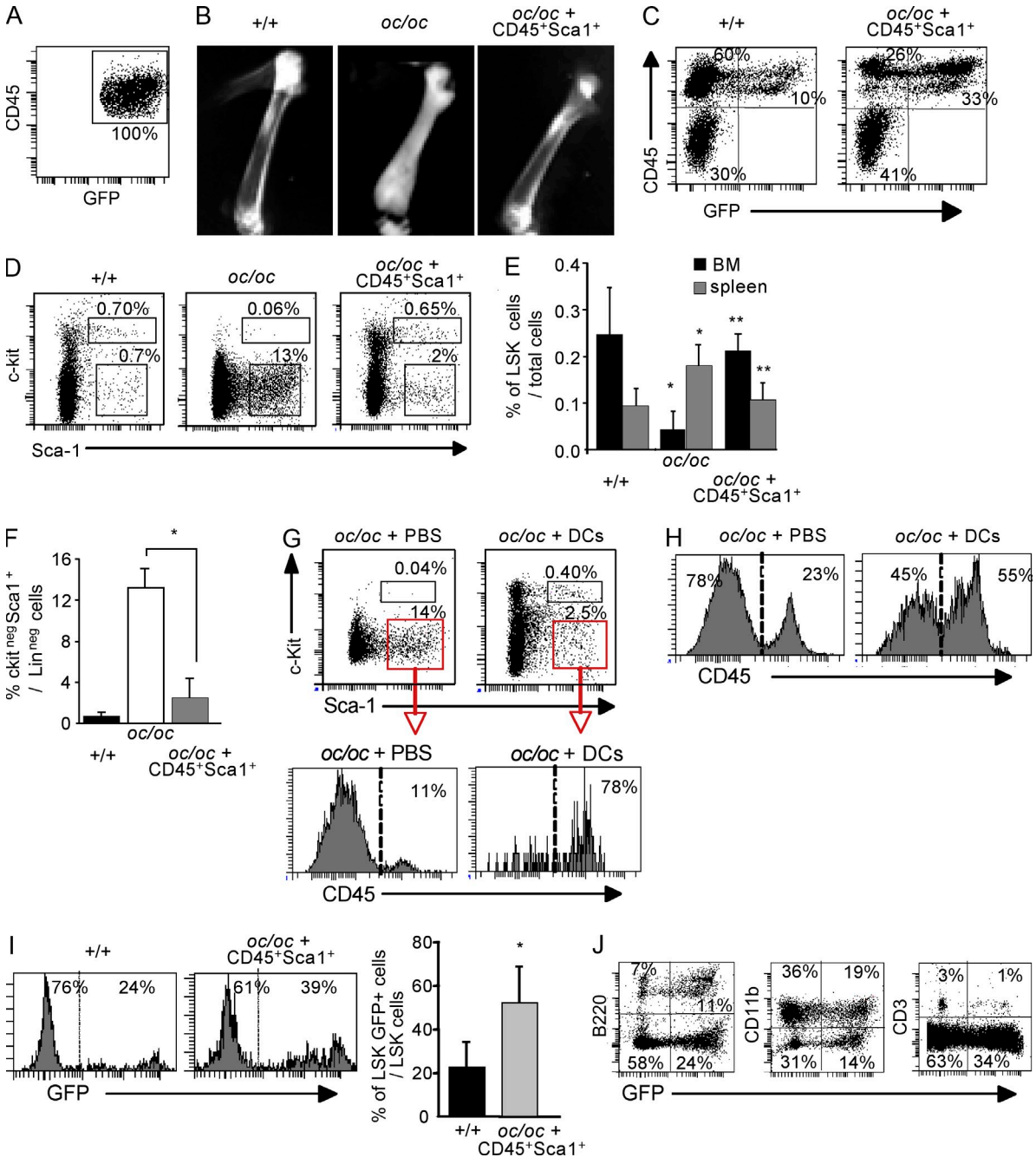

Figure 5. Restoration of OCL activity rescues LSK homing in the BM of *oc/oc* mice. Sorted CD45$^+$Sca1$^+$ hematopoietic progenitors from actin-GFP (3–4-wk-old) mice were transferred into newborn *oc/oc* and wild-type mice. Analyses were performed at day 45 for the wild-type and treated *oc/oc* mice (*oc/oc* + CD45$^+$Sca1$^+$), and at day 17 for the untreated *oc/oc* mice because of their short life span. (A) Typical FACS profile of sorted GFP$^+$CD45$^+$Sca1$^+$ cells before transfer into irradiated recipient mice. (B) Radiological analysis of the femur of treated and control mice, representative of four mice per group in two independent experiments. (C) Flow cytometry analysis of CD45 and GFP expression in the BM of the wild-type and treated *oc/oc* mice. Percentage of the cells in each quadrant is indicated. Data are representative four mice in each group in two independent experiments. (D) Flow cytometry analysis of LSK cells in the BM of the treated +/+ and *oc/oc* mice and control untreated *oc/oc* mice. Cells were gated on Lin^{neg} cells. Percentages of the populations are indicated. Data are representative four mice per group in two independent experiments. (E) Bar graph shows the mean ± SD of the percentage of LSK cells in the BM and the spleen obtained for four mice per group in two independent experiments. *, $P < 0.01$ (+/+ versus control *oc/oc* mice); **, $P < 0.01$ (treated *oc/oc* versus control *oc/oc* mice). (F) Mean ± SD of the percentage of Sca1$^+$c-kit^{neg} cells in Lin^{neg} cells from the BM and the spleen of four mice per group in two independent experiments. *, $P < 0.01$. (G) Flow cytometry analysis on BM LSK cells of 17-d-old PBS- or DC-treated *oc/oc* mice gated on lin^{neg} cells (top) and on CD45 expression gated on BM Lin^{neg}Sca1$^+$c-kit^{neg} cells (bottom). Data are representative of those obtained for three mice per group in one experiment. (H) Flow cytometry analysis of BM Ter119^{neg}CD45^{neg} mesenchymal cells. Data are representative of those

macrophages, which are both involved in HSC retention in their niche (Winkler et al., 2010; Chow et al., 2011), was increased in the BM of *oc/oc* mice compared with control (Fig. 4, C and D). These results indicate that the decrease in HSC numbers in the *oc/oc* BM is not related to a reduction of perivascular mesenchymal cells or macrophage populations.

Recovering OCL activity in *oc/oc* mice restores LSK homing to the BM

The *Tcirg1* gene mutated in *oc/oc* mice is not expressed in mesenchymal cells and in HSCs (unpublished data; Schinke et al., 2009). Thus, the profound changes observed both in mesenchymal and hematopoietic cell populations are likely to be caused by the absence of OCL activity rather than by a cell autonomous effect of the *oc* mutation on mesenchymal and LSK cells.

We have therefore assessed whether restoring OCL activity in *oc/oc* mice could reestablish both the bone phenotype and the formation of the HSC niche in the BM. OCLs derive from the monocyte lineage, and the transfer of hematopoietic cells restores OCL activity in *oc/oc* mice (Seifert and Marks, 1987; Frattini et al., 2005; Johansson et al., 2006; Wakkach et al., 2008). Thus, we corrected OCL activity in *oc/oc* mice by adoptive transfer of $Sca1^+$ hematopoietic progenitors from actin-GFP mice. To avoid any contamination by $CD45^{neg}$ mesenchymal cells, the injected hematopoietic progenitors were sorted as the $CD45^+Sca1^+GFP^+$ cells (Fig. 5 A). Analysis of the mouse phenotype was performed at day 45 in the wild-type and the treated *oc/oc* mice, caused by the time required to reach restoration of the bone turnover (Wakkach et al., 2008; Mansour et al., 2011), and at day 17 in the untreated *oc/oc* mice because of their short life span up to 21 d (Blin-Wakkach et al., 2006a). As expected and already described (Frattini et al., 2005; Johansson et al., 2006), this treatment induced a restoration of bone resorption as supported by the formation of a BM cavity that was absent in *oc/oc* mice (Fig. 5 B). No GFP^+CD45^{neg} cells were present in the treated mice, confirming that no donor mesenchymal cells were transferred (Fig. 5 C). The proportion of LSK cells in the BM of treated *oc/oc* mice (Fig. 5 D) dramatically increased compared with that of the untreated mice (Fig. 5, D and E), eventually reaching the level observed in the wild-type mice. Simultaneously, the proportion of LSK cells in the spleen of treated *oc/oc* mice decreased to the level found in the wild-type mice (Fig. 5 E). Importantly, the changes in the localization of LSK cells were associated with a decrease in the $Lin^{neg}Sca1^+cKit^{neg}$ cells that also became equivalent to the level observed in the wild-type mice (Fig. 5, D and F). A similar restoration of the LSK and mesenchymal cell compartments was also observed in *oc/oc* mice treated with +/+ dendritic cells (Fig. 5, G and H) that have been recently shown to efficiently differentiate into functional OCLs in this model (Wakkach et al., 2008). This observation confirmed that this restoration is specifically linked to the recovering of OCL activity and not to another hematopoietic cell modification.

Analysis of the LSK cells present in the BM of *oc/oc* mice treated with $CD45^+Sca1^+GFP^+$ cells revealed that they were both from the donor (LSK GFP^+) and the recipient (LSK GFP^{neg}) mice (Fig. 5 I). This result reveals that endogenous *oc/oc* LSK cells have a normal capacity to home to the BM, and that their dramatic decrease was caused by the defective niche and not by a cell autonomous impairment in their homing capacity. Furthermore, both the donor and recipient hematopoietic progenitors were able to generate cells of the main hematopoietic lineages in the treated *oc/oc* mice, indicating that LSK cells in these mice have normal differentiation potential (Fig. 5 J). Altogether, these data clearly demonstrated that the restoration of OCL function has corrected the deficient LSK cell homing in *oc/oc* BM.

Restoring OCL activity in *oc/oc* mice reestablishes the formation of the HSC niche

To determine whether this restoration of LSK cell homing in the BM was caused by the restoration of the mesenchymal cell phenotype, we have further analyzed the $TER119^{neg}CD45^{neg}$ cells in the *oc/oc* mice treated with $CD45^+Sca1^+GFP^+$. The percentage of the $TER119^{neg}CD45^{neg}$ cells in the treated *oc/oc* mice was decreased compared with the untreated *oc/oc* mice and returned to the level observed in the wild-type mice (Fig. 6 A). Moreover, this decrease was found within the $CD45^{neg}$ $Sca1^+$ fraction (Fig. 5, D and F; and Fig. 6 B) suggesting that the mesenchymal cells in the $TER119^{neg}$ population from the treated-*oc/oc* mice have differentiated into a more mature phenotype.

To further evaluate the recovery of the mesenchymal cell phenotype and OBL differentiation and function, histological and gene expression analysis were performed. Histological analysis using Von Gieson's staining showed that the *oc/oc* BM is filled with bone tissue containing large zones of cartilage and type I collagen (Fig. 6 C, blue and pink staining, respectively) as previously described (Seifert and Marks, 1985; Wakkach et al., 2008). This altered bone phenotype revealed an impaired endochondral ossification that probably participated in the alteration of the HSC niche in the BM. In contrast, in the treated *oc/oc* mice, the bone structure was similar to the one observed in the wild-type mice with a normal BM cavity and a reduced amount of cartilage compared with the

obtained for three mice per group in one experiment. (I) Analysis of GFP expression in LSK cells from the wild-type and *oc/oc* mice treated with $CD45^+Sca1^+GFP^+$ cells. Cells were gated on BM LSK cells. Bar graph shows the mean ± SD of the percentage of GFP^+LSK cells obtained for four mice per group in two independent experiments. *, $P < 0.05$. (J) Flow cytometry analysis of the main hematopoietic lineages (B220 for B cells, CD11b for monocytes, and CD3 for T cells) in the BM of *oc/oc* mice treated with $CD45^+Sca1^+GFP^+$ cells. Percentage of cells in each quadrant is indicated. Data are representative of four treated *oc/oc* mice in two independent experiments.

untreated *oc/oc* mice, indicating a restoration of a normal bone formation (Fig. 6 C). This finding was confirmed by RT-PCR analysis showing that the expression of OBL markers also returned to a normal level (Fig. 6 D). Furthermore, the expression of the main factors important for the niche function was also equivalent to the levels observed in the wild-type control mice. These results strongly supported an interaction between OCLs and OBL precursors that contribute to the formation of the HSC niche in normal mice. Therefore, we performed double staining of tartrate-resistant acid phosphatase (TRAP), a marker of OCLs, and ALP, a marker of early OBLs and osteoid formation. In the trabecular zone of +/+ mice, most of OCLs were juxtaposed with early ALP$^+$ OBLs (Fig. 6 E). On the contrary, in *oc/oc* mice, the ALP labeling was dramatically decreased (Fig. 6 F), as previously described (Mansour et al., 2011), because of the decreased OBL commitment. However, early ALP$^+$ OBLs were detected in some regions of the BM; most of them were isolated from OCLs (Fig. 6 G). This result confirmed a potential interaction between OCLs and early OBLs, which is abolished in *oc/oc* mice. Interestingly, the juxtaposition between OCLs and early OBLs was restored in treated *oc/oc* mice, confirming that the interaction between these cells had been corrected by the restoration of OCL activity (Fig. 6 H). Together with

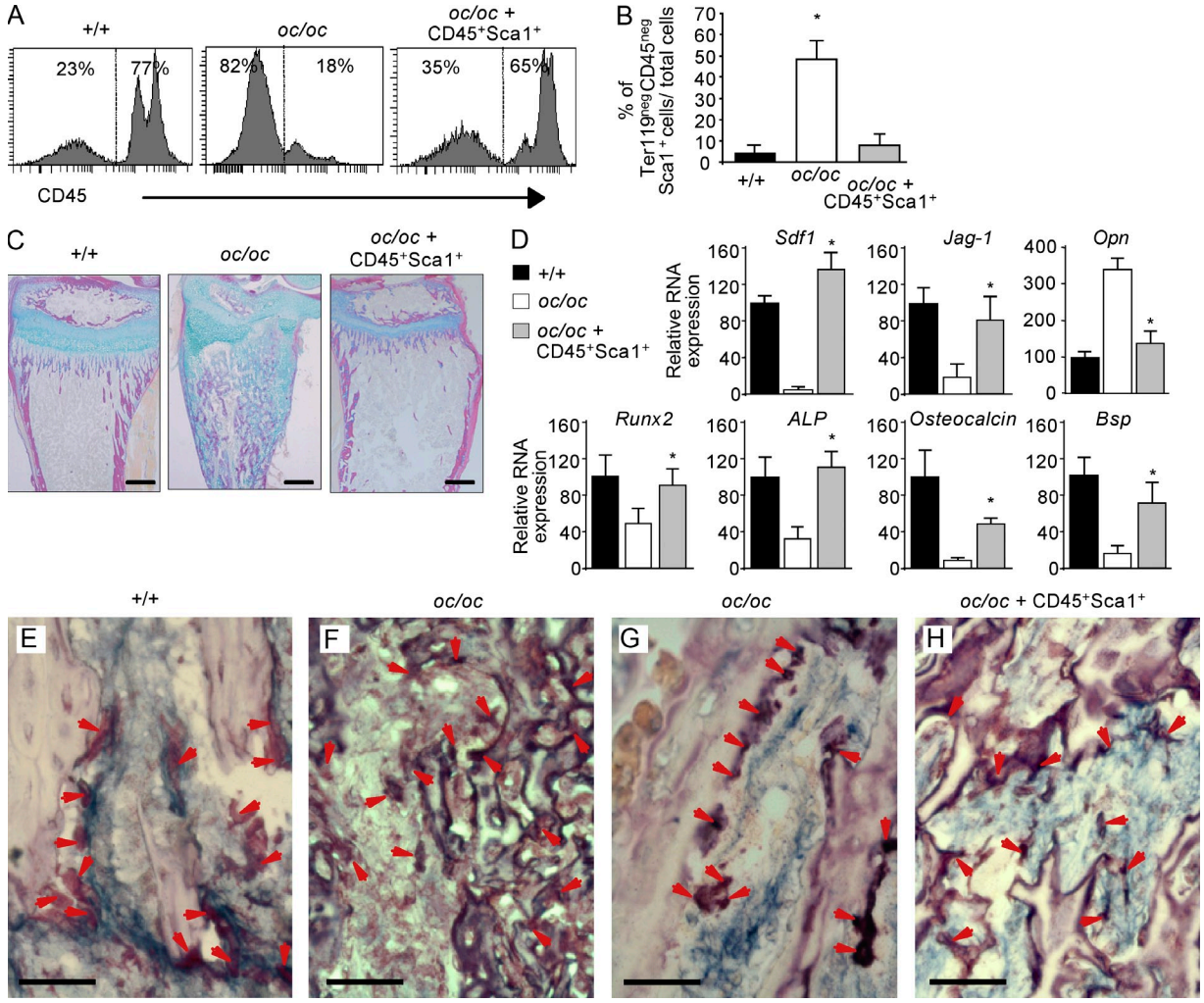

Figure 6. Restoration of OCL activity rescues the mesenchymal phenotype in the BM of *oc/oc* mice. (A) Flow cytometry analysis of CD45 expression in Ter119^{neg} BM cells from control and *oc/oc* mice treated with CD45$^+$Sca1$^+$GFP$^+$ cells presented in Fig. 4. Cells were gated on Ter119^{neg} cells. Data are representative of four mice per group in two independent experiments. (B) Mean ± SD of the percentage of Ter119^{neg}CD45^{neg} Sca1$^+$ cells in the BM of four mice per group and representative of two independent experiments. *, $P < 0.01$. (C) Histological analysis of the tibia after Van Gieson and Alcian blue staining; type 1 collagen (pink) and cartilage (blue). Bars, 200 µm. Data are representative of two mice per group in two independent experiments. (D) RT-PCR analysis of CD45^{neg} cells from treated and control mice. Ct values were normalized to the 36B4 RNA. Differences were calculated with the $2^{-\Delta Ct}$ method and expressed as percentage relative to the values obtained for the wild-type cells. Results are presented as the mean ± SD of triplicates from four mice in each group and are representative of two independent experiments. *, $P < 0.01$ (treated *oc/oc* versus control *oc/oc* mice). (E–H) Histological analysis on the BM of +/+ mice (E), *oc/oc* mice (F and G), and treated *oc/oc* mice (H) using purple TRAP staining for OCLs (arrows) and blue ALP staining for osteoblastic cells. Data are representative of three mice per group in two independent experiments. Bars, 50 µm.

the increased proportion of LSK cells (Fig. 4, D and E), these data demonstrate that restoring OCL activity not only rescued the commitment and maturation of OBLs but also restored their function as providers of hematopoietic niches, probably through cellular interactions between OCLs and early OBLs.

DISCUSSION

The present studies establish a novel aspect of the role of bone cells in the initial formation of the HSC niche in the BM and demonstrated that OCLs play a critical role in this formation. We demonstrate for the first time that in the absence of OCL activity, the BM HSC niche formation is severely affected and mesenchymal cells have a highly reduced capacity to attract hematopoietic progenitors, leading to an impaired homing of these progenitors. Furthermore, we show that restoration of OCL activity reverses this phenotype and allows normal hematopoietic progenitor homing in the BM.

The shift of hematopoiesis to the BM occurs just before birth and is preceded by endochondral ossification and OCL activity (Aguila and Rowe, 2005). During this process, the initial unmineralized and mineralized cartilage is gradually degraded by OCLs and replaced by the bone matrix produced by OBLs (Mackie et al., 2008). In *oc/oc* mice, this process is altered because of the absence of OCL activity, and long bones display a defect in bone matrix formation characterized by the persistence of large areas of mineralized and unmineralized cartilage (Banco et al., 1985; Seifert and Marks, 1985; Wakkach et al., 2008). Here, we showed that this alteration in endochondral ossification is caused by an impaired OBL differentiation from mesenchymal progenitors in the *oc/oc* BM, as revealed by the dramatic decrease in the expression of the OBL markers *Runx2*, *Alp*, *Osteocalcin*, and *Bsp* and the reduced proportion of cells expressing CD51 and the integrin α5 (CD49e), both of which are traits associated with OBL commitment (Lundberg et al., 2007; Hamidouche et al., 2009). This is in agreement with our recent studies demonstrating that the generation of CFU-ALP (representing OBL-committed cells) from *oc/oc* BM is very low compared with controls and that the number of ALP-producing cells is significantly reduced in vivo in the *oc/oc* bone (Mansour et al., 2011).

Different mesenchymal cells have been implicated in the HSC niche, including immature and perivascular primitive mesenchymal cells (Morikawa et al., 2009; Méndez-Ferrer et al., 2010), osteoprogenitors (Raaijmakers et al., 2010), and OBLs (Nilsson et al., 2001; Calvi et al., 2003; Zhang et al., 2003; Visnjic et al., 2004), but their relative role in the HSC niche is still a matter of debate (Askmyr et al., 2009; Ehninger and Trumpp, 2011; Lévesque and Winkler, 2011). In *oc/oc* mice, the percentage of $Lin^{neg}CD45^{neg}Sca1^{+}$ mesenchymal progenitor cells is dramatically increased in the BM, a result that is in agreement with our previous finding of a high number of CFU-F (representing mesenchymal progenitors) generated from *oc/oc* BM cells (Mansour et al., 2011). Furthermore, the proportion of $TER119^{neg}CD45^{neg}Sca1^{+}PDGFR\alpha^{+}$ cells described as perivascular primitive mesenchymal cells being part of the HSC niche in adults (Morikawa et al., 2009) is also increased. Thus, the impaired HSC niche formation observed in *oc/oc* mice is not caused by a defect in mesenchymal progenitors and perivascular mesenchymal cells, indicating that these cells are not sufficient for this formation and that another essential actor is altered in these mice. In this sense, the correlation between the impaired OBL commitment and the dramatic reduction in BM HSC number strongly indicated that osteoblastic cells are required for the formation of the HSC niche. This was further supported by the effect of treatment with ZA on the HSC niche in newborn mice. Interestingly, we previously reported that, in adults, blockade of OCL activity by ZA reduced OBL commitment and increased mesenchymal progenitors without affecting the LSK cell compartment (Mansour et al., 2011). These observations suggest that the OBLs are less important for the maintenance of the HSC niche in adults than for its formation in newborns, and that the OCL effect on the HSC niche reported here is specific to the initial formation of the niche, but is probably not involved in latter stages.

The reduced expression of the key regulators of HSC expansion, quiescence, homing, and maintenance (such as Jag-1, Ang-1, and SDF1) found in *oc/oc* $CD45^{neg}$ mesenchymal cells, as well as their reduced ability to attract hematopoietic progenitors, are most likely involved in the impaired progenitor homing and responsible for the loss of HSCs in the *oc/oc* BM. In addition, because OPN was described as a negative regulator of the niche and was shown to down-regulate the expression of *Jag-1* and *Ang-1* (Stier et al., 2005), the high expression of OPN in the *oc/oc* mesenchymal cells may also contribute to the reduced HSC number in the *oc/oc* BM.

Importantly, the alteration of both the HSC niche and OBL commitment is not self-autonomous, as the mutated *Tcirg1* gene in *oc/oc* mice is not expressed in mesenchymal cells (Schinke et al., 2009) and the restoration of OCL activity allows recovery of the OBL commitment and normal bone and hematopoietic niche formation. Collectively, these data point out that OCLs act as the key regulators of all these processes.

Previous studies have identified OCLs and phagocytic cells from the same lineage (macrophages) as regulators of the mobilization of HSCs outside of their BM niches in adult mice. Stimulation of OCL activity induces HSC mobilization and hematopoietic progenitor expansion mediated by the production of proteolytic enzymes that degrade components of the HSC niche (such as SDF-1 or SCF) required for stem cell anchorage and retention (Kollet et al., 2006). The same effect has also been observed when OCL differentiation and function are inhibited, without reduction of OBL number and function (Lymperi et al., 2011; Miyamoto et al., 2011). Moreover, the depletion of macrophages induces the mobilization of HSCs outside of the BM. This mobilization is associated with a reduction in the expression of SDF1, Ang-1, and stem cell factor (SCF) and involves modification in the phenotype of either perivascular mesenchymal stem

cells (Chow et al., 2011) or OBLs (Winkler et al., 2010; Christopher et al., 2011). All these data indicate that once the HSC niche is formed, OCLs and phagocytic cells play an important role in regulating HSC maintenance in this niche. This role is probably dependent on both the proteolytic activity of these cells and the crosstalk signals with OBLs, but the precise mechanisms involved remained to be determined. In *oc/oc* mice, the BM macrophages were not decreased, ruling out a possible effect of macrophage depletion in this model. Our results point out a novel function of active OCLs that is clearly different from those mentioned at the beginning of the paragraph. Indeed, the previously reported role of OCLs deals with the modulation of HSC egress from a "mature" HSC niche in adults, whereas our data demonstrate the importance of OCLs in the initial niche formation and in its colonization by LSK cells through the stimulation of OBL commitment.

Recently, analysis in osteopetrotic models, in particular in *op/op* mice defective in M-CSF and in OCL function, reported that LSK mobilization in response to G-CSF is unaffected or even increases (Miyamoto et al., 2011). But the maintenance of LSK cells in the BM of these mice was not clearly established. Indeed, despite the observation of HSCs in the BM of *op/op* mice (Miyamoto et al., 2011), their number remains 10-fold lower than in control mice (Begg et al., 1993) and no data were reported in the other osteopetrotic models (Miyamoto et al., 2011). Moreover, despite HSC maintenance in *op/op* mice (Miyamoto et al., 2011), the authors have excluded the spleen as a site for the high number of stem cells observed in their livers suggests that hematopoiesis may be maintained in this organ after birth (Wiktor-Jedrzejczak et al., 1982). Therefore, together with our results, all these data suggest that in osteopetrotic models, the colonization of the BM by HSCs may be impaired, explaining why OCLs have no effect on their mobilization.

In *oc/oc* mice, OCLs are present but inactive, thus their effect on the formation of the HSC niche is clearly dependent on their bone resorbing activity; our results demonstrated that their effect is linked to their capacity to support OBL commitment. Therefore, the mean by which OCLs control the formation of the HSC niche is likely to depend on coupling or cell adhesion factors produced during bone resorption, and on participating in the interaction between OCLs, OBLs, and their progenitors (Martin and Sims, 2005; Tang et al., 2009). The cross talk between bone resorption and bone formation may be achieved through various mechanisms. Indeed, coupling factors such as insulin-like growth factor, basic fibroblast growth factor, TGF-β, bone morphogenetic proteins, and platelet-derived growth factor are released from the bone matrix during bone resorption and are known to induce bone formation, thereby coupling bone resorption and formation (Sims and Gooi, 2008). Active OCLs also produce acid and proteases that activate the coupling factors, e.g., TGF-β1. Recently, it has been shown that the release and activation of TGF-β1 in response to osteoclastic bone resorption induces migration of mesenchymal precursor cells to the resorptive sites and their differentiation into OBLs (Tang et al., 2009). It was also reported that blockage of OCL activity by bisphosphonates inhibits the release of active TGF-β1 and the recruitment of Sca-1^+ skeletal stem cells for the bone formation (Tang et al., 2009). In this sense, we observed in the *oc/oc* BM a reduced juxtaposition between OCLs and early OBLs that is corrected after restoration of OCL activity. Such a phenotype probably involves reduced expression of molecules involved in the contact between OCLs and osteoblastic cells. Interestingly, the expression of c-kit and its ligand Kit-L is dramatically reduced in the *oc/oc* BM. The c-Kit–Kit-L pathway is a potent stimulator of cell adhesion involved not only in the maintenance of HSCs, but also in the adhesion between OCLs and OBLs (Gattei et al., 1996; Lotinun et al., 2005). Therefore, the decreased expression of both c-kit and its ligand could participate in a reduced communication between OCLs and osteoblastic cells that could be involved in the defect in the HSC niche observed in *oc/oc* mice.

Although the specific mechanisms involved in this cross talk between OCLs and OBL progenitors leading to HSC niche formation remains to be elucidated, a reduced production of coupling factors or adhesion factors in *oc/oc* mice may result in an impaired OBL commitment and HSC niche formation. Lastly, in addition to their effect on OBLs, OCLs may also act directly on HSC homing through calcium released from the bone matrix, which is also a potent regulator of HSC retention in close physical proximity to the endosteal surface, interacting with the calcium-sensing receptors expressed on HSCs (Adams et al., 2006).

In conclusion, we show here for the first time that active OCLs are necessary for the initial formation of the HSC niche. The loss of OCL-resorbing activity blocks the cellular and molecular interactions in the BM and ultimately disrupts the niche formation through the loss of endosteal OBLs, thereby inhibiting the colonization of the BM by HSCs. These findings extend our knowledge of the processes participating in the establishment of the HSC niche, which is critical in understanding normal and pathological hematopoiesis.

MATERIALS AND METHODS

Mice and treatment. Osteopetrotic *oc/oc* mice (C57BL/6J X C3HheB/FeJ genetic background) were obtained by crossing heterozygous *oc/+* mice. Genotyping was performed as previously described (Blin-Wakkach et al., 2004b). Analyses were performed on 17-d-old *oc/oc* mice and control +/+ littermates. Transgenic mice expressing GFP under the control of the actin promoter (actin-GFP mice) were obtained from C. Mueller (Institut de Biologie Moléculaire et Cellulaire, Strasbourg, France). Pregnant C57BL/6 females received an intraperitoneal injection of 100 µg/kg ZA (Novartis) in 100 µl PBS or 100 µl PBS alone (control mice) 3 d a week for the duration of their pregnancy. From the day of birth, the newborn mice issued from ZA-treated females also received intraperitoneal injection of 100 µg/kg ZA in 50 µl PBS, whereas those from PBS-treated females received PBS alone, 3 d a week. Analyses were performed on 15-d-old PBS- or ZA-treated mice. All animals were maintained in our central animal facility in accordance with the general guidelines of the Direction des Services Vétérinaires.

Approval for the use of mice in this study was obtained from the animal facility committee from the Faculty of Medicine at the University of Nice Sophia Antipolis.

Flow cytometry analysis. BM cells from 17-d-old *oc/oc* mice and control +/+ littermates were collected by crushing the femora into small pieces and vigorous pipetting, as previously described (Blin-Wakkach et al., 2004a,b). Splenocytes were isolated by filtration through a 40-µm cell strainer (BD). Blood cells were obtained by intracardiac puncture, as previously described (Augier et al., 2010). After red blood cell lysis, HSCs were analyzed after exclusion of lineage (Lin)-positive cells using FITC-conjugated antibodies against Ly76 (Ter-119), CD3 (17A2), CD11b (M1/70), and B220 (RA3-6B2) and after labeling with Sca1 (D7) and c-kit (288) antibodies. For mesenchymal cell analysis, cells were labeled with antibodies against CD45 (30F11), Ly76 (Ter-119), Sca1, CD44 (IM7), CD49e (5H1Q-275), CD51 (RMV-7; all from BD), and PDGFRα (APA5; eBioscience). For macrophage analysis, cells were labeled with antibodies against CD11b (M1/70), F4/80 (Cl:A3-1), Ly6G (1A8), Gr1 (RB6-8C5), CD115 (AFS98; all from BD), and CD169 (3D6.112; AbD Serotec). After washes, the labeled cells were analyzed on a FACSCanto (BD). For cell purification, $CD45^{neg}$ mesenchymal cells were sorted on a cell sorter (FACSAria; BD) with high purity (>99%).

RNA expression analysis. Total RNA was extracted from the purified $CD45^{neg}$ cells by adsorption onto silica membranes (Macherey-Nagel) as previously described (Blin-Wakkach et al., 2004a,b). Total RNA (1 µg) was reverse transcribed with random primers according to the manufacturer's protocol (Invitrogen). Real-time PCR analysis was performed on an ABI Prism 7000 (Applied Biosystems), in a 20-µl volume containing 10-fold diluted cDNA, 10 µl SYBR Green Master Mix, and 300 nM of each primer. Samples were treated according to the following program: 5°C for 2 min, 94°C for 10 min, and 40 cycles of 95°C for 15 s and 60°C for 1 min. Analyses were performed in triplicate. For each sample, the cycle threshold (Ct) values were determined. Test cDNA results were normalized to the ribosomic 36B4 RNA on the same plate. Differences in gene expression between *oc/oc* and control mice were calculated using the 2ΔCt method. At the end of the PCR assay, generating a melting curve of the PCR product and analysis by gel electrophoresis controlled the specificity of amplification. The following primers were used: *Sdf1*, 5′-GAGCCAACGTCAAGCATCTG-3′ and 5′-CGGGTCAATGCACACTTGT-3′; *N-Cad*: 5′-TCCCTTATCTCCA-GTGACTATTAAAAGA-3′ and 5′-TCTTTAAATTGAGCTGAGCAAA-ATCA-3′; *Ang-1*, 5′-GAAGCAACAACTGGAGCTCATG-3′ and 5′-TCCT-CCCTTTAGCAAAACACCTT-3′; *Jag-1*, 5′-AACGACCGTAATCGC-ATCGT-3′ and 5′-TATCAGGTTGAATAGTGTCATTACTGGAA-3′; *Kit-l*, 5′-TCCGAAGAGGCCAGAAACTAG-3′ and 5′-CTAAGGGAGCTG-GCTGCAA-3′; *Opn*, 5′-CTGTGTCCTCTGAAGAAAAGGATG-3′ and 5′-GCTTTCATTGGAATTGCTTGG-3′; *36B4*, 5′-TCCAGGCTTTGGG-CATCA-3′ and 5′-CTTTATCAGCTGCACATCACTCAGA-3′; *Osteocalcin*, 5′-CCACCCGGGAGCAGTGT-3′ and 5′-CTAAATAGTGATACCG-TAGATGCGTTTG-3′; *Runx2*, 5′-TTTAGGGCGCATTCCTCATC-3′ and 5′-TGTCCTTGTGGATTAAAAGGACTTG-3′; *Bone sialoprotein (BSP)*, 5′-CCAAGCACAGACTTTTGAGTTAGC-3′ and 5′-CTTTCTGCATC-TCCAGCCTTCT-3′; *Alkaline phosphatase* (*ALP*), 5′-TCAGGGCAAT-GAGGTCACATC-3′ and 5′-CACAATGCCCACGGACTTC-3′.

HSC homing and migration assays. BM cells from 3–4-wk-old actin-GFP mice were enriched in $Sca1^+$ cells using Sca1 microbeads (Miltenyi Biotech) according to the manufacturer protocol. From these $Sca1^+$-enriched cells, $CD45^+$ LSK GFP^+ cells were sorted (FACSAria; BD) with high purity sorting (>99%). For in vivo homing analysis, these cells were injected intraperitoneally (2.5×10^5 cells in 50 µl PBS) into 2-d-old *oc/oc* or +/+ mice after nonlethal total body irradiation (3Gy). Animals were sacrificed after 18 h, and the presence of GFP^+ progenitor cells was analyzed by flow cytometry (FACSCanto; BD). For in vitro migration assay, $CD45^{neg}$ cells were sorted from the BM of *oc/oc* and +/+ mice on a cell sorter (FACSAria; BD). 10^6 $CD45^{neg}$ cells were placed in MEMα medium containing 5% fetal calf serum (HyClone) and incubated at 37°C and 5% CO_2 in the bottom chamber of 5-µm pore size transwells (Costar). After 24 h, 5×10^4 LSK GFP^+ cells were added in the top chamber in MEMα medium. After 3 h of incubation at 37°C and 5% CO_2, cells that had migrated into the bottom chamber were collected and the number of GFP^+ cells was determined by flow cytometry.

$Sca1^+$ cell engraftment in *oc/oc* mice. $Sca1^+CD45^+$ cells were sorted from the BM of 3–4-wk-old actin-GFP mice (FACSAria; BD), with high purity (100%). These cells were injected intraperitoneally (5×10^6 cells in 50 µl PBS) into 2-d-old *oc/oc* or +/+ irradiated mice (3Gy) as previously described (Wakkach et al., 2008) and animals were sacrificed at day 45. The untreated *oc/oc* mice were sacrificed at day 17, because of their short life span (Blin-Wakkach et al., 2006a), and used as the control. For treatment with DCs, $CD11c^+$MHC-II^+ DCs were sorted from +/+ mice and were transferred (5×10^6 cells) intraperitoneally into 2-d-old *oc/oc* irradiated mice (3Gy), as previously described (Wakkach et al., 2008).

Histological analysis. For histological analysis of the tibia, undecalcified bones were fixed in 4% paraformaldehyde, dehydrated, and embedded in methylmethacrylate, as previously described (Wakkach et al., 2008). 7-µm sections were stained with a 0.3% Alcian blue in 3% acetic acid solution and, subsequently, with Van Gieson's solution. Acquisitions were performed using a microscope (model DMLB; Leica), and a 3CCD color video DXC-390 camera (Sony). For OCL and early OBL analysis, femora were fixed in 4% paraformaldehyde for 24 h at 4°C, decalcified for 10 d in 10% EDTA at 4°C and incubated overnight in a 30% glucose solution. 8-µm bone sections were stained for ALP activity with the leukocyte alkaline phosphatase kit (fast blue BB salt; Sigma-Aldrich), and then for TRAP activity with the leukocyte acid phosphatase kit (Sigma-Aldrich), according to the manufacturer's protocol. After hematoxylin staining, images were acquired on an Observer Z1 inverted microscope and an AxioCam lCc1 8-Bit Color camera (both from Carl Zeiss, Inc.).

We thank M. Topi for animal care and technical assistance. We thank C. Mueller (IBMC, Strasbourg, France) for the kind gift of actin-GFP mice. We thank R. Dacquin (LBMC, Centre National de la Recherche Scientifique UMR 5161, Lyon, France) for Van Gieson's analysis. We also greatly acknowledge the cell imaging facility of the Centre Méditérranéen de Médecine Moléculaire, Nice, France (MICA plateform), the flow cytometry facility, and the PETC transcriptomic facility both from Institut National de la Santé et de la Recherche Médicale UMR 576, Nice.

This work was supported by the Ministère de l'enseignement et de la Recherche (A. Mansour).

The authors have no competing financial interests.

Submitted: 16 May 2011
Accepted: 18 January 2012

REFERENCES

Adams, G.B., and D.T. Scadden. 2006. The hematopoietic stem cell in its place. *Nat. Immunol.* 7:333–337. http://dx.doi.org/10.1038/ni1331

Adams, G.B., K.T. Chabner, I.R. Alley, D.P. Olson, Z.M. Szczepiorkowski, M.C. Poznansky, C.H. Kos, M.R. Pollak, E.M. Brown, and D.T. Scadden. 2006. Stem cell engraftment at the endosteal niche is specified by the calcium-sensing receptor. *Nature.* 439:599–603. http://dx.doi.org/10.1038/nature04247

Aguila, H.L., and D.W. Rowe. 2005. Skeletal development, bone remodeling, and hematopoiesis. *Immunol. Rev.* 208:7–18. http://dx.doi.org/10.1111/j.0105-2896.2005.00333.x

Arai, F., A. Hirao, M. Ohmura, H. Sato, S. Matsuoka, K. Takubo, K. Ito, G.Y. Koh, and T. Suda. 2004. Tie2/angiopoietin-1 signaling regulates hematopoietic stem cell quiescence in the bone marrow niche. *Cell.* 118:149–161. http://dx.doi.org/10.1016/j.cell.2004.07.004

Askmyr, M., N.A. Sims, T.J. Martin, and L.E. Purton. 2009. What is the true nature of the osteoblastic hematopoietic stem cell niche? *Trends Endocrinol. Metab.* 20:303–309. http://dx.doi.org/10.1016/j.tem.2009.03.004

Augier, S., T. Ciucci, C. Luci, G.F. Carle, C. Blin-Wakkach, and A. Wakkach. 2010. Inflammatory blood monocytes contribute to tumor development and represent a privileged target to improve host immunosurveillance. *J. Immunol.* 185:7165–7173. http://dx.doi.org/10.4049/jimmunol.0902583

Banco, R., M.F. Seifert, S.C. Marks Jr., and J.L. McGuire. 1985. Rickets and osteopetrosis: the osteosclerotic (oc) mouse. *Clin. Orthop. Relat. Res.* (201):238–246.

Begg, S.K., J.M. Radley, J.W. Pollard, O.T. Chisholm, E.R. Stanley, and I. Bertoncello. 1993. Delayed hematopoietic development in osteopetrotic (op/op) mice. *J. Exp. Med.* 177:237–242. http://dx.doi.org/10.1084/jem.177.1.237

Blin-Wakkach, C., A. Wakkach, N. Rochet, and G.F. Carle. 2004a. Characterization of a novel bipotent hematopoietic progenitor population in normal and osteopetrotic mouse. *J. Bone Miner. Res.* 19:1137–1143. http://dx.doi.org/10.1359/JBMR.040318

Blin-Wakkach, C., A. Wakkach, P.M. Sexton, N. Rochet, and G.F. Carle. 2004b. Hematological defects in the *oc/oc* mouse, a model of infantile malignant osteopetrosis. *Leukemia.* 18:1505–1511. http://dx.doi.org/10.1038/sj.leu.2403449

Blin-Wakkach, C., V. Breuil, D. Quincey, C. Bagnis, and G.F. Carle. 2006a. Establishment and characterization of new osteoclast progenitor cell lines derived from osteopetrotic and wild type mice. *Bone.* 39:53–60. http://dx.doi.org/10.1016/j.bone.2005.12.078

Blin-Wakkach, C., A. Wakkach, D. Quincey, and G.F. Carle. 2006b. Interleukin-7 partially rescues B-lymphopoiesis in osteopetrotic oc/oc mice through the engagement of B220+ CD11b+ progenitors. *Exp. Hematol.* 34:851–859. http://dx.doi.org/10.1016/j.exphem.2006.04.003

Calvi, L.M., G.B. Adams, K.W. Weibrecht, J.M. Weber, D.P. Olson, M.C. Knight, R.P. Martin, E. Schipani, P. Divieti, F.R. Bringhurst, et al. 2003. Osteoblastic cells regulate the haematopoietic stem cell niche. *Nature.* 425:841–846. http://dx.doi.org/10.1038/nature02040

Chan, C.K., C.C. Chen, C.A. Luppen, J.B. Kim, A.T. DeBoer, K. Wei, J.A. Helms, C.J. Kuo, D.L. Kraft, and I.L. Weissman. 2009. Endochondral ossification is required for haematopoietic stem-cell niche formation. *Nature.* 457:490–494. http://dx.doi.org/10.1038/nature07547

Cho, K.A., S.Y. Joo, H.S. Han, K.H. Ryu, and S.Y. Woo. 2010. Osteoclast activation by receptor activator of NF-kappaB ligand enhances the mobilization of hematopoietic progenitor cells from the bone marrow in acute injury. *Int. J. Mol. Med.* 26:557–563.

Chow, A., D. Lucas, A. Hidalgo, S. Méndez-Ferrer, D. Hashimoto, C. Scheiermann, M. Battista, M. Leboeuf, C. Prophete, N. van Rooijen, et al. 2011. Bone marrow CD169+ macrophages promote the retention of hematopoietic stem and progenitor cells in the mesenchymal stem cell niche. *J. Exp. Med.* 208:261–271. http://dx.doi.org/10.1084/jem.20101688

Christopher, M.J., M. Rao, F. Liu, J.R. Woloszynek, and D.C. Link. 2011. Expression of the G-CSF receptor in monocytic cells is sufficient to mediate hematopoietic progenitor mobilization by G-CSF in mice. *J. Exp. Med.* 208:251–260. http://dx.doi.org/10.1084/jem.20101700

Dar, A., O. Kollet, and T. Lapidot. 2006. Mutual, reciprocal SDF-1/CXCR4 interactions between hematopoietic and bone marrow stromal cells regulate human stem cell migration and development in NOD/SCID chimeric mice. *Exp. Hematol.* 34:967–975. http://dx.doi.org/10.1016/j.exphem.2006.04.002

Dougall, W.C., M. Glaccum, K. Charrier, K. Rohrbach, K. Brasel, T. De Smedt, E. Daro, J. Smith, M.E. Tometsko, C.R. Maliszewski, et al. 1999. RANK is essential for osteoclast and lymph node development. *Genes Dev.* 13:2412–2424. http://dx.doi.org/10.1101/gad.13.18.2412

Ehninger, A., and A. Trumpp. 2011. The bone marrow stem cell niche grows up: mesenchymal stem cells and macrophages move in. *J. Exp. Med.* 208:421–428. http://dx.doi.org/10.1084/jem.20110132

Frattini, A., H.C. Blair, M.G. Sacco, F. Cerisoli, F. Faggioli, E.M. Catò, A. Pangrazio, A. Musio, F. Rucci, C. Sobacchi, et al. 2005. Rescue of ATPa3-deficient murine malignant osteopetrosis by hematopoietic stem cell transplantation in utero. *Proc. Natl. Acad. Sci. USA.* 102:14629–14634. http://dx.doi.org/10.1073/pnas.0507637102

Gattei, V., D. Aldinucci, J.M. Quinn, M. Degan, M. Cozzi, V. Perin, A.D. Iuliis, S. Juzbasic, S. Improta, N.A. Athanasou, et al. 1996. Human osteoclasts and preosteoclast cells (FLG 29.1) express functional c-kit receptors and interact with osteoblast and stromal cells via membrane-bound stem cell factor. *Cell Growth Differ.* 7:753–763.

Hamidouche, Z., O. Fromigué, J. Ringe, T. Häupl, P. Vaudin, J.C. Pagès, S. Srouji, E. Livne, and P.J. Marie. 2009. Priming integrin alpha5 promotes human mesenchymal stromal cell osteoblast differentiation and osteogenesis. *Proc. Natl. Acad. Sci. USA.* 106:18587–18591. http://dx.doi.org/10.1073/pnas.0812334106

Johansson, M., L. Jansson, M. Ehinger, A. Fasth, S. Karlsson, and J. Richter. 2006. Neonatal hematopoietic stem cell transplantation cures oc/oc mice from osteopetrosis. *Exp. Hematol.* 34:242–249. http://dx.doi.org/10.1016/j.exphem.2005.11.010

Kollet, O., A. Dar, S. Shivtiel, A. Kalinkovich, K. Lapid, Y. Sztainberg, M. Tesio, R.M. Samstein, P. Goichberg, A. Spiegel, et al. 2006. Osteoclasts degrade endosteal components and promote mobilization of hematopoietic progenitor cells. *Nat. Med.* 12:657–664. http://dx.doi.org/10.1038/nm1417

Kollet, O., A. Dar, and T. Lapidot. 2007. The multiple roles of osteoclasts in host defense: bone remodeling and hematopoietic stem cell mobilization. *Annu. Rev. Immunol.* 25:51–69. http://dx.doi.org/10.1146/annurev.immunol.25.022106.141631

Kong, Y.Y., H. Yoshida, I. Sarosi, H.L. Tan, E. Timms, C. Capparelli, S. Morony, A.J. Oliveira-dos-Santos, G. Van, A. Itie, et al. 1999. OPGL is a key regulator of osteoclastogenesis, lymphocyte development and lymph-node organogenesis. *Nature.* 397:315–323. http://dx.doi.org/10.1038/16852

Lévesque, J.P., and I.G. Winkler. 2011. Hierarchy of immature hematopoietic cells related to blood flow and niche. *Curr. Opin. Hematol.* 18:220–225. http://dx.doi.org/10.1097/MOH.0b013e3283475fe7

Lévesque, J.P., F.M. Helwani, and I.G. Winkler. 2010. The endosteal 'osteoblastic' niche and its role in hematopoietic stem cell homing and mobilization. *Leukemia.* 24:1979–1992. http://dx.doi.org/10.1038/leu.2010.214

Lotinun, S., G.L. Evans, R.T. Turner, and M.J. Oursler. 2005. Deletion of membrane-bound steel factor results in osteopenia in mice. *J. Bone Miner. Res.* 20:644–652. http://dx.doi.org/10.1359/JBMR.041209

Lundberg, P., S.J. Allison, N.J. Lee, P.A. Baldock, N. Brouard, S. Rost, R.F. Enriquez, A. Sainsbury, M. Lamghari, P. Simmons, et al. 2007. Greater bone formation of Y2 knockout mice is associated with increased osteoprogenitor numbers and altered Y1 receptor expression. *J. Biol. Chem.* 282:19082–19091. http://dx.doi.org/10.1074/jbc.M609629200

Lymperi, S., A. Ersek, F. Ferraro, F. Dazzi, and N.J. Horwood. 2011. Inhibition of osteoclast function reduces hematopoietic stem cell numbers in vivo. *Blood.* 117:1540–1549. http://dx.doi.org/10.1182/blood-2010-05-282855

Mackie, E.J., Y.A. Ahmed, L. Tatarczuch, K.S. Chen, and M. Mirams. 2008. Endochondral ossification: how cartilage is converted into bone in the developing skeleton. *Int. J. Biochem. Cell Biol.* 40:46–62. http://dx.doi.org/10.1016/j.biocel.2007.06.009

Mansour, A., A. Anginot, S.J.C. Mancini, C. Schiff, G.F. Carle, A. Wakkach, and C. Blin-Wakkach. 2011. Osteoclast activity modulates B-cell development in the bone marrow. *Cell Res.* 21:1102–1115. http://dx.doi.org/10.1038/cr.2011.21

Martin, T.J., and N.A. Sims. 2005. Osteoclast-derived activity in the coupling of bone formation to resorption. *Trends Mol. Med.* 11:76–81. http://dx.doi.org/10.1016/j.molmed.2004.12.004

Méndez-Ferrer, S., T.V. Michurina, F. Ferraro, A.R. Mazloom, B.D. Macarthur, S.A. Lira, D.T. Scadden, A. Ma'ayan, G.N. Enikolopov, and P.S. Frenette. 2010. Mesenchymal and haematopoietic stem cells form a unique bone marrow niche. *Nature.* 466:829–834. http://dx.doi.org/10.1038/nature09262

Miyamoto, K., S. Yoshida, M. Kawasumi, K. Hashimoto, T. Kimura, Y. Sato, T. Kobayashi, Y. Miyauchi, H. Hoshi, R. Iwasaki, et al. 2011. Osteoclasts are dispensable for hematopoietic stem cell maintenance and mobilization. *J. Exp. Med.* 208:2175–2181. http://dx.doi.org/10.1084/jem.20101890

Morikawa, S., Y. Mabuchi, Y. Kubota, Y. Nagai, K. Niibe, E. Hiratsu, S. Suzuki, C. Miyauchi-Hara, N. Nagoshi, T. Sunabori, et al. 2009. Prospective identification, isolation, and systemic transplantation of

multipotent mesenchymal stem cells in murine bone marrow. *J. Exp. Med.* 206:2483–2496. http://dx.doi.org/10.1084/jem.20091046

Nagasawa, T., S. Hirota, K. Tachibana, N. Takakura, S. Nishikawa, Y. Kitamura, N. Yoshida, H. Kikutani, and T. Kishimoto. 1996. Defects of B-cell lymphopoiesis and bone-marrow myelopoiesis in mice lacking the CXC chemokine PBSF/SDF-1. *Nature.* 382:635–638. http://dx.doi.org/10.1038/382635a0

Nilsson, S.K., H.M. Johnston, and J.A. Coverdale. 2001. Spatial localization of transplanted hemopoietic stem cells: inferences for the localization of stem cell niches. *Blood.* 97:2293–2299. http://dx.doi.org/10.1182/blood.V97.8.2293

Nilsson, S.K., H.M. Johnston, G.A. Whitty, B. Williams, R.J. Webb, D.T. Denhardt, I. Bertoncello, L.J. Bendall, P.J. Simmons, and D.N. Haylock. 2005. Osteopontin, a key component of the hematopoietic stem cell niche and regulator of primitive hematopoietic progenitor cells. *Blood.* 106:1232–1239. http://dx.doi.org/10.1182/blood-2004-11-4422

Peled, A., I. Petit, O. Kollet, M. Magid, T. Ponomaryov, T. Byk, A. Nagler, H. Ben-Hur, A. Many, L. Shultz, et al. 1999. Dependence of human stem cell engraftment and repopulation of NOD/SCID mice on CXCR4. *Science.* 283:845–848. http://dx.doi.org/10.1126/science.283.5403.845

Raaijmakers, M.H., S. Mukherjee, S. Guo, S. Zhang, T. Kobayashi, J.A. Schoonmaker, B.L. Ebert, F. Al-Shahrour, R.P. Hasserjian, E.O. Scadden, et al. 2010. Bone progenitor dysfunction induces myelodysplasia and secondary leukaemia. *Nature.* 464:852–857. http://dx.doi.org/10.1038/nature08851

Russell, R.G., N.B. Watts, F.H. Ebetino, and M.J. Rogers. 2008. Mechanisms of action of bisphosphonates: similarities and differences and their potential influence on clinical efficacy. *Osteoporos. Int.* 19:733–759. http://dx.doi.org/10.1007/s00198-007-0540-8

Schinke, T., A.F. Schilling, A. Baranowsky, S. Seitz, R.P. Marshall, T. Linn, M. Blaeker, A.K. Huebner, A. Schulz, R. Simon, et al. 2009. Impaired gastric acidification negatively affects calcium homeostasis and bone mass. *Nat. Med.* 15:674–681. http://dx.doi.org/10.1038/nm.1963

Scimeca, J.C., A. Franchi, C. Trojani, H. Parrinello, J. Grosgeorge, C. Robert, O. Jaillon, C. Poirier, P. Gaudray, and G.F. Carle. 2000. The gene encoding the mouse homologue of the human osteoclast-specific 116-kDa V-ATPase subunit bears a deletion in osteosclerotic (oc/oc) mutants. *Bone.* 26:207–213. http://dx.doi.org/10.1016/S8756-3282(99)00278-1

Seifert, M.F., and S.C. Marks Jr. 1985. Morphological evidence of reduced bone resorption in the osteosclerotic (oc) mouse. *Am. J. Anat.* 172:141–153. http://dx.doi.org/10.1002/aja.1001720204

Seifert, M.F., and S.C. Marks Jr. 1987. Congenitally osteosclerotic (oc/oc) mice are resistant to cure by transplantation of bone marrow or spleen cells from normal littermates. *Tissue Cell.* 19:29–37. http://dx.doi.org/10.1016/0040-8166(87)90054-1

Sims, N.A., and J.H. Gooi. 2008. Bone remodeling: Multiple cellular interactions required for coupling of bone formation and resorption. *Semin. Cell Dev. Biol.* 19:444–451. http://dx.doi.org/10.1016/j.semcdb.2008.07.016

Stier, S., Y. Ko, R. Forkert, C. Lutz, T. Neuhaus, E. Grünewald, T. Cheng, D. Dombkowski, L.M. Calvi, S.R. Rittling, and D.T. Scadden. 2005. Osteopontin is a hematopoietic stem cell niche component that negatively regulates stem cell pool size. *J. Exp. Med.* 201:1781–1791. http://dx.doi.org/10.1084/jem.20041992

Tagaya, H., T. Kunisada, H. Yamazaki, T. Yamane, T. Tokuhisa, E.F. Wagner, T. Sudo, L.D. Shultz, and S.I. Hayashi. 2000. Intramedullary and extramedullary B lymphopoiesis in osteopetrotic mice. *Blood.* 95:3363–3370.

Takamatsu, Y., P.J. Simmons, R.J. Moore, H.A. Morris, L.B. To, and J.P. Lévesque. 1998. Osteoclast-mediated bone resorption is stimulated during short-term administration of granulocyte colony-stimulating factor but is not responsible for hematopoietic progenitor cell mobilization. *Blood.* 92:3465–3473.

Tang, Y., X. Wu, W. Lei, L. Pang, C. Wan, Z. Shi, L. Zhao, T.R. Nagy, X. Peng, J. Hu, et al. 2009. TGF-beta1-induced migration of bone mesenchymal stem cells couples bone resorption with formation. *Nat. Med.* 15:757–765. http://dx.doi.org/10.1038/nm.1979

Visnjic, D., Z. Kalajzic, D.W. Rowe, V. Katavic, J. Lorenzo, and H.L. Aguila. 2004. Hematopoiesis is severely altered in mice with an induced osteoblast deficiency. *Blood.* 103:3258–3264. http://dx.doi.org/10.1182/blood-2003-11-4011

Wakkach, A., A. Mansour, R. Dacquin, E. Coste, P. Jurdic, G.F. Carle, and C. Blin-Wakkach. 2008. Bone marrow microenvironment controls the in vivo differentiation of murine dendritic cells into osteoclasts. *Blood.* 112:5074–5083. http://dx.doi.org/10.1182/blood-2008-01-132787

Wiktor-Jedrzejczak, W.W., A. Ahmed, C. Szczylik, and R.R. Skelly. 1982. Hematological characterization of congenital osteopetrosis in op/op mouse. Possible mechanism for abnormal macrophage differentiation. *J. Exp. Med.* 156:1516–1527. http://dx.doi.org/10.1084/jem.156.5.1516

Winkler, I.G., N.A. Sims, A.R. Pettit, V. Barbier, B. Nowlan, F. Helwani, I.J. Poulton, N. van Rooijen, K.A. Alexander, L.J. Raggatt, and J.P. Lévesque. 2010. Bone marrow macrophages maintain hematopoietic stem cell (HSC) niches and their depletion mobilizes HSCs. *Blood.* 116:4815–4828. http://dx.doi.org/10.1182/blood-2009-11-253534

Zhang, J., C. Niu, L. Ye, H. Huang, X. He, W.G. Tong, J. Ross, J. Haug, T. Johnson, J.Q. Feng, et al. 2003. Identification of the haematopoietic stem cell niche and control of the niche size. *Nature.* 425:836–841. http://dx.doi.org/10.1038/nature02041